

# Immunosuppressive Cyclosporin A Activates AKT in Keratinocytes through PTEN Suppression

## IMPLICATIONS IN SKIN CARCINOGENESIS\*

Received for publication, June 1, 2009, and in revised form, January 19, 2010. Published, JBC Papers in Press, February 12, 2010, DOI 10.1074/jbc.M109.028142

Weinong Han<sup>‡</sup>, Mei Ming<sup>‡</sup>, Tong-Chuan He<sup>§</sup>, and Yu-Ying He<sup>‡1</sup>

From the <sup>‡</sup>Section of Dermatology, Department of Medicine, and <sup>§</sup>Department of Surgery, University of Chicago, Chicago, Illinois 60637

Non-melanoma skin cancer, the most common neoplasia after solid organ transplantation, causes serious morbidity and mortality and is related to sun exposure. Cyclosporin A (CsA) has been used widely to prevent rejection in organ transplantation. The mechanism of CsA action in causing cancer was thought to be well understood via immunosuppression. Here, we show that CsA promotes primary skin tumor growth in immune-deficient mice and keratinocyte growth *in vitro*. In addition, CsA enhances keratinocyte survival from removal of extracellular matrix or UVB radiation. At the molecular level, CsA increases AKT activation after serum treatment and UVB irradiation. Furthermore we found that expression of PTEN, the negative regulator of AKT activation, is significantly reduced post-CsA in human HaCaT and A431 cells and in mouse skin *in vivo*. CsA-induced PTEN down-regulation occurs at the transcription level and is epidermal growth factor receptor-dependent. Such PTEN suppression is required for increased AKT activation. Inhibition of AKT activation abolishes CsA-promoted growth and survival, indicating that AKT hyperactivation is essential for both growth and survival of CsA-treated cells. In addition, mTOR signaling as a known AKT downstream pathway is required for CsA-enhanced growth and survival. Taken together, we have identified the PTEN/AKT pathway as new molecular targets of CsA in epidermal keratinocytes, suggesting a previously unknown mechanism in CsA-enhanced skin carcinogenesis. Our findings challenge assumptions about how CsA-associated tumors arise in skin.

Skin cancer is the most common cancer in the United States. A population that is particularly at high risk is organ transplant recipients, a growing subset of our population due to increased graft survival and numbers of graft recipients. Skin cancers are the most common malignant conditions in transplant recipients. With the development of new immunosuppressive agents, the majority of transplant recipients can survive for decades, and malignancy has become a major burden on long term survival. For example, the cumulative incidence of skin cancer in transplant recipients in Queensland, Australia, increases from

7% after 1 year of immunosuppressive therapy to 82% after 20 years. Among skin cancers, squamous cell carcinoma (SCC)<sup>2</sup> is the most common skin cancer, occurring 65–250 times as frequently as in the general population (1). In addition, SCCs appear to be more aggressive in transplant recipients than in the general population.

Many organ transplant recipients are given the drug cyclosporin A (CsA) to suppress their immune system. Extensive clinical studies have shown that the lifetime course of such treatment causes a dramatic increase in risk of skin cancer as a major adverse effect (1–3). CsA increases the skin cancer risk, always thought to be a side effect of the depressed immune system.

Ultraviolet (UV) exposure in patients taking immunosuppressant drugs is a major environmental risk factor for skin cancer. UV radiation in sunlight reaching the Earth's surface is composed of UVB (280–315 nm) and UVA (315–400 nm). In animal models, UV radiation is a complete carcinogen that can initiate and promote skin carcinogenesis, resulting in SCC, basal cell carcinoma, and melanoma (4–7). Enhanced cell survival, incomplete DNA repair, and immune suppression after UV radiation are critical for skin carcinogenesis (8, 9). In organ transplant recipients, skin cancer development depends on the duration of immunosuppressive treatment and UV exposure history after (or even before) transplantation. SCCs occur even in children with organ transplantation, suggesting that immunosuppressive treatment accelerates skin carcinogenesis (3).

Phosphatase and tensin homolog deleted on chromosome 10 (PTEN) is a negative regulator of AKT signaling and functions as a tumor suppressor (10, 11). This discovery places PTEN into a mechanistically critical position. Loss of PTEN function results in increased AKT activation (12). The critical role of functional PTEN suppression in skin malignancies has been confirmed in humans and mice. Hereditary heterozygous mutation of PTEN in humans is associated with Cowden syndrome (13), a disorder characterized by the onset of multiple hamartomas in various tissues including the skin. Skin-condi-

\* This work was supported by the American Skin Association, the Wendy Will Case Cancer Fund, University of Chicago Comprehensive Cancer Center Grant P30 CA014599, Clinical and Translational Science Award UL1RR024999, and the University of Chicago "Friends of Dermatology" endowment fund.

<sup>1</sup> To whom correspondence should be addressed. Tel.: 773-795-4696; Fax: 773-702-8398; E-mail: yyhe@medicine.bsd.uchicago.edu.

<sup>2</sup> The abbreviations used are: SCC, squamous cell carcinoma; AG, AG1478, an EGFR kinase inhibitor; PI3K, phosphatidylinositol 3-kinase; AKT, a serine-threonine kinase, downstream of PI3K, also called protein kinase B; CsA, cyclosporin A; EGFR, epidermal growth factor receptor; ERK, extracellular signal-regulated kinase; EV, empty vector; LY, LY294002, a PI3K/AKT inhibitor; mTOR, the mammalian target of rapamycin; PTEN, phosphatase and tensin homolog deleted on chromosome 10; RNAi, small interfering RNA (siRNA); shRNA, short hairpin RNA; UVA, ultraviolet A (315–400 nm); UVB, ultraviolet B (280–315 nm); NC, negative control; FBS, fetal bovine serum; DN, dominant negative; MTS, 3-(4,5-dimethylthiazol-2-yl)-5-(3-carboxymethoxyphenyl)-2,4-sulfophenyl-2H-tetrazolium, inner salt.

## Cyclosporin A Activates AKT

tional PTEN knock-out (k5Ptenflox/flox) mice develop spontaneous tumors (14).

It has long been considered that immunosuppression is the only factor in the increased skin cancer in organ transplant recipients. However, the action of CsA on keratinocytes may play an important role. This action may also explain why skin cancer is the dominant form of cancer developed in these patients and may provide a molecular basis for better preventive strategies. In this study we seek to determine the direct effect of CsA on epidermal keratinocytes and the molecular and cellular mechanisms involved in CsA-associated skin carcinogenesis.

### MATERIALS AND METHODS

**Cell Culture, UVB Treatment, Adenoviral Infection, Immunohistochemistry, and Immunoprecipitation**—HaCaT, A431, or HeLa (ATCC) cells were cultured in 60-mm dishes with normal culture medium. For UVB treatment, the Stratagene 2400 equipped with 312-nm UVB bulbs (Stratagene, La Jolla, CA) (UVC, 0%, UVB 51%, and UVA 49%) was used. The UV exposure was performed in phosphate-buffered saline (PBS) after washing the cells with PBS twice to avoid the photosensitization effect of components in culture medium on the cells. In selected experiments, cells were preincubated with inhibitors at 37 °C for 1 h before irradiation. Inhibitors used were AG1478 (AG), LY294002 (LY), and rapamycin (Biomol, Plymouth Meeting, PA). After UVB treatment, cells were incubated at 37 °C with or without the inhibitors. Adenoviral infection was performed as described previously (15–17). Immunohistochemistry analysis was performed by the Core facility at the University of Chicago. PTEN levels were evaluated in basal keratinocytes of the interfollicular epidermis. At least 50 keratinocytes were selected for analysis of PTEN levels by ImageJ (National Institutes of Health).

**CsA Treatment and Tumor Formation after Inoculation into Nude Mice**—HaCaT and A431 cells were treated with CsA at predetermined concentrations or DMSO (0.001%, as vehicle control). To determine tumor growth of A431 cells treated with or without CsA, separate groups (six mice each group) of nude mice (Harlan Sprague-Dawley) were inoculated subcutaneously with one million A431 cells using Matrigel as described previously (18). In the CsA group, mice were treated daily with CsA (20 mg/kg body weight) by gavage starting 1 day before tumor cell injection. Tumor formation and growth were assessed every other day. Separate groups of mice ( $n = 3$ ) were treated with CsA or vehicle daily for 30 days. At the end of the studies, mice were euthanized. Skin (and tumor) tissues were collected; half were fixed in formalin, and half were snap-frozen in liquid nitrogen.

**siRNA and shRNA Transfection**—Transfection of cells with siRNA or shRNA was performed as described previously (16, 19). An ON-TARGETplus SMARTpool siRNA targeting PTEN (Dharmacon, l-003023) was used, which included four duplexes. Their target sequences are GAUCAGCAUACACA-AAUUA, GACUUAGACUUGACCUAUA, GAUCUUGACC-AAUGGCUAA, and CGAUAGCAUUUGCAGUAUA. The sequences for PTEN shRNAs are GAGACAGACTGATGTG-

TATAC (i-1) (Origene, TR200219) and CGTATAC AGGAA-CAATATTG (i-2, Addgene Plasmid10669) (20).

**Determination of Apoptosis by Flow Cytometry**—Apoptosis was determined by staining cells with annexin V/propidium iodide (PI) or fixed cells with PI followed by flow cytometry, as described previously (15, 21).

**Determination of Cell Viability**—Cells were incubated for 48 h in non-tissue culture Petri dishes that do not support cell attachment and then transferred to tissue culture dishes to allow survived cells to attach. Twenty-four hours later, cell viability was measured using the MTS assay (CellTiter 96Aqueous Proliferation Assay Promega) and monitored at 492 nm using a TECAN Infinite M200 plate reader according to the manufacturer's instructions.

**Western Blotting**—Western blotting was performed as described previously (19–21). Antibodies used were as follows: PTEN (Santa Cruz Biotechnology), p-AKT (phospho-AKT-Ser-473, and phospho-AKT-Thr-308, Cell Signaling Technology), p-ERK (phospho-ERK1/2, Santa Cruz), p-EGFR (phospho-EGFR-tyrosine 1173, Santa Cruz), AKT (AKT1, AKT2, AKT3, and AKT1/2/3, Santa Cruz), ERK (Santa Cruz), EGFR (NeoMarker), hemagglutinin (Santa Cruz), and  $\beta$ -actin (Santa Cruz). The optical density of the scanned blot was quantified using ImageJ relative to a standard titration curve of PTEN protein. Data were expressed as percentage, with the protein level in the control taken to be 100%.

**Real-time PCR**—Quantitative real time PCR assays were performed using ABI7300 (Applied Biosystems, Foster City, CA). Real-time reverse transcription-PCR fluorescence detection was performed in 96-well plates with the SYBR<sup>®</sup> Green PCR Master Mix (Applied Biosystems) as described previously (22). Amplification primers were 5'-AGTTCCTCAGCCGT-TACCT-3' (forward) 5'-AGGTTTCCTCTGGTCCTGGT-3' (reverse) for the *PTEN* gene and 5'-ACTGGAACGGTGAAG-GTGACA-3' (forward) and 5'-ATGGCAAGGGACTTCCTG-TAAC-3' (reverse) for  $\beta$ -actin. The threshold cycle number ( $C_T$ ) for each sample was determined in triplicate. The  $C_T$  for values for PTEN were normalized against  $\beta$ -actin as described previously (22).

**Luciferase Reporter Assays**—HaCaT cells were seeded in 6-well plates and grown to 50–60% confluence. The plasmid mixtures, containing 1  $\mu$ g of PTEN promoter luciferase construct (PTEN-Luc in pGL3 vector, kindly provided by Ian de Belle at the Burnham Institute of Medical Research) and 0.025  $\mu$ g of pRL-TK (Promega, used as a transfection efficiency control), were transfected using FuGENE 6 transfection reagent (Roche Applied Science) according to the manufacturer's protocol. The empty vector pGL3 was used as a vector control. At 48 h after transfection, the cells were harvested in 1 $\times$  luciferase lysis buffer (Promega), and luciferase activity was measured with a TD-20/20 Luminometer (Turner BioSystems) and normalized with the values of pRL-TK luciferase activity using a dual luciferase reporter assay kit (DLR, Promega).

**Statistical Analyses**—Data were expressed as the mean of three independent experiments and analyzed by Student's *t* test and analysis of variance. A two-sided value of  $p < 0.05$  was considered significant in all cases.

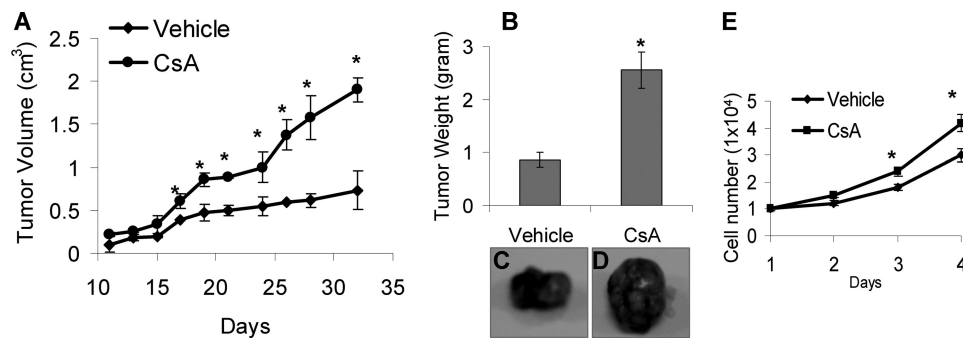


**FIGURE 1. CsA increases tumor growth of A431 cells in nude mice and promotes keratinocyte growth *in vitro*.** *A*, nude mice (6/group) were treated with CsA (20 mg/kg of body weight) or vehicle (olive oil, 200  $\mu$ l). The next day A431 cells treated with vehicle (DMSO, 0.001%) or CsA (250 ng/ml) for 3 days were injected subcutaneously into the mice. The mice were continuously treated with CsA daily until the end of the study. *Days* shows the days after cell injection. *B*, tumor weight at the end of the study is shown. *C* and *D*, representative pictures of tumors from mice treated with or without CsA are shown. *E*, cells ( $1 \times 10^4$ ) were seeded in 96-well plates and cultured for different times. Cell growth was determined by an MTS assay. \*,  $p < 0.05$ , significant difference from cells or mice treated without CsA.

## RESULTS

**CsA Increases Growth of A431 Cells in Nude Mice**—To determine the direct effect of CsA on keratinocytes, we first examined the effect of CsA on tumor growth of human epidermoid A431 SCC cells in nude mice, which do not have an immune system for CsA to suppress. CsA was dissolved in olive oil and administered by gavage 1 day before tumor cell inoculation. The treatment was continued daily at 20 mg/kg of body weight. In the CsA-treated group, A431 cells were pretreated with CsA (250 ng/ml) for 72 h before inoculation. The selection of this *in vitro* CsA concentration is based on the plasma levels of standard CsA therapy in organ transplant recipients (23).

A431 cells grew tumors in nude mice (Fig. 1*A*). The tumors developed in the CsA-treated group grew significantly faster than those in vehicle-treated counterparts ( $p < 0.05$ ). The tumors were much larger than those in vehicle-treated mice in weight and in size ( $p < 0.05$ ; Fig. 1, *B–D*). As nude mice do not have the immune system for CsA to suppress, these data indicate that CsA promotes immunosuppression-independent growth of A431 cells *in vivo*.

**CsA Promotes Growth of Keratinocytes *in Vitro***—To determine whether CsA directly affects cell growth *in vitro*, we analyzed the difference in growth of cells with or without CsA treatment. We established CsA-treated keratinocytes by culturing human HaCaT keratinocytes in the presence of CsA at different concentrations (0, 100, 250, or 1000 ng/ml) for 16 weeks. This treatment regimen is based on the clinical data that SCCs in CsA-treated organ transplant recipients take years to develop, indicating that the increased SCC incidence requires cumulative and chronic CsA treatment. We selected HaCaT cells as the cellular model to examine the molecular mechanisms of CsA-enhanced skin carcinogenesis, because HaCaT cells are not tumorigenic but possess UV-type p53 mutations (24) and, therefore, have been used widely as a UV-initiated cellular model to evaluate skin tumor promotion and progression caused by UV and other factors. Indeed, p53 mutations are detectable in normal non-tumor skin in humans (25). We found that CsA-treated cells grew significantly faster than vehicle-treated cells at 3 and 4 days ( $p < 0.05$ ) but not at 1 and 2 days after plating the

same number of cells (Fig. 1*E*). These findings demonstrate that CsA directly promotes growth of HaCaT keratinocytes.

**CsA Promotes Survival of Keratinocytes**—To further determine the effect of CsA on epidermal keratinocytes, we examined whether CsA has an effect on survival of keratinocytes, which is critical to eliminate damaged cells.

We first examined cell survival upon removal of the extracellular matrix. CsA-treated or vehicle-treated cells were trypsinized and plated on non-tissue culture Petri dishes. This type of dish prevents cells from attaching and, therefore, forces them into suspension. 24 and 48 h later, cells were collected. Cells grown in regular dishes and attached to the dishes were used as controls. No apoptosis was detected at 24 h after removal of the extracellular matrix. However, removal of the extracellular matrix for 48 h without exposure to CsA induced apoptosis in 40% of the cells compared with control cells in which only 7.8% were apoptotic (Fig. 2*A*). CsA at 100 ng/ml significantly reduced apoptotic cells to 17%, and CsA at 250 ng/ml reduced apoptotic cells to 15% ( $p < 0.05$ ). MTS assays indicated that CsA at 100 and 250 but not 1000 ng/ml significantly inhibited apoptosis ( $p < 0.05$ ; Fig. 2*B*). These data indicate that CsA protects cells from apoptosis induced by loss of the extracellular matrix.

Next we determined the effect of CsA on UV-induced apoptosis in keratinocytes. UV damage is associated with increased skin cancer risk in organ transplant recipients (3). Apoptosis in response to UVB is critical to eliminate damaged cells. We used annexin V and sub-G<sub>1</sub> assays to measure apoptosis. In CsA-treated cells, 20 mJ/cm<sup>2</sup> UVB-induced apoptosis was slightly lower than in vehicle-treated cells (Fig. 2, *C* and *D*). In control cells, however, 30 mJ/cm<sup>2</sup> UVB induced 37% apoptosis, whereas only about 7% apoptosis was detected in cells treated with CsA (100 or 250 ng/ml) ( $p < 0.05$ ; Fig. 2, *C* and *D*). In addition, we determined apoptosis by staining fixed cells with propidium iodide and then analyzed the sub-G<sub>1</sub> population as shown by the arrow (Fig. 2*E*). There was no apoptosis for cells kept in the dark. When cells were exposed to UVB (25 mJ/cm<sup>2</sup>), 16% cells were apoptotic in control cells, whereas only about 7% of cells underwent apoptosis in CsA-treated cells ( $p < 0.05$ ; Fig. 2, *E* and *F*). These data indicate that CsA protects keratinocytes from UVB-induced apoptosis.

**CsA Enhances AKT Activation upon Serum Treatment or UVB Radiation and Down-regulates PTEN**—AKT hyperactivation plays an important role in cell growth and survival and is negatively regulated by the tumor suppressor PTEN (12). To determine the molecular mechanisms of CsA-promoted cell growth and survival, we analyzed the effect of CsA on AKT activation and PTEN levels. CsA (100, 250, or 1000 ng/ml) increased AKT phosphorylation at serine 473 at 24 and 48 h after incubation with 10% fetal bovine serum (FBS) ( $p < 0.05$ ;

## Cyclosporin A Activates AKT

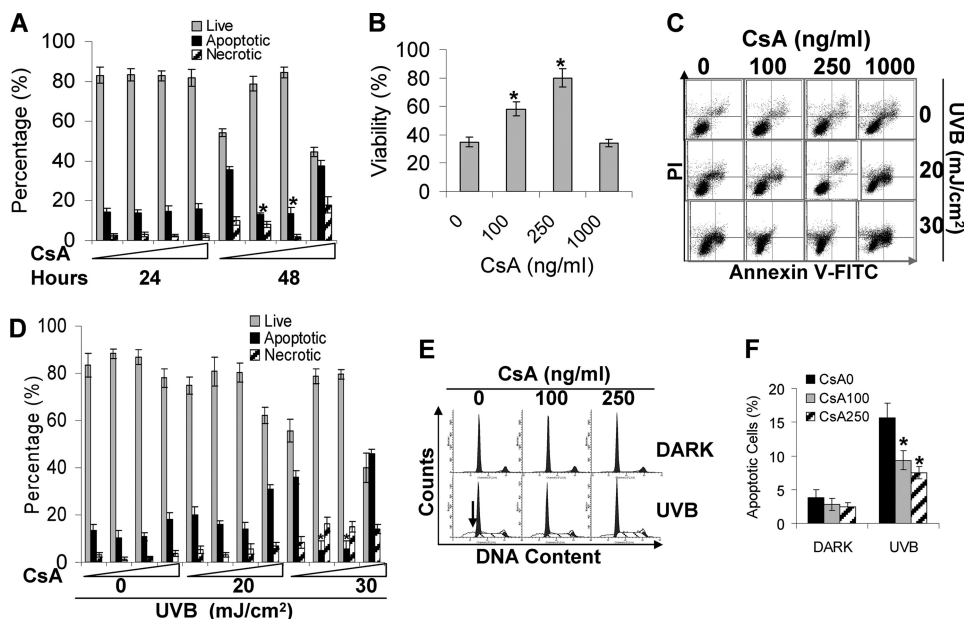


**FIGURE 2. CsA inhibits apoptosis.** *A*, cells treated with CsA (0, 100, and 250 ng/ml) for 16 weeks were trypsinized and plated in non-tissue culture dishes. 24 or 48 h later, cells were collected and stained with TACS™ annexin V kits (Trevigen), and apoptosis was determined by flow cytometry. *B*, cell survival was determined by MTS assay at 48 h after the cells lost their extracellular matrix by seeding them in regular tissue culture dishes and then incubating for 24 h. *C*, cells treated with vehicle or CsA (100, 250, or 1000 ng/ml) were exposed to UVB. Eighteen hours after UVB, cells were collected for annexin V/propidium iodide (PI) assay as in *A*. *D*, quantification of live, apoptotic, and necrotic cells from *A* is shown. *E*, cell apoptosis was analyzed by propidium iodide as indicated by the sub-G<sub>1</sub> population. *F*, quantification of sub-G<sub>1</sub> population. \*,  $p < 0.05$ , significant difference from cells treated without CsA. FITC, fluorescein isothiocyanate.

Fig. 3, *A* and *B*). In screening the mechanisms of CsA-enhanced AKT activation, we found that CsA significantly down-regulated PTEN ( $p < 0.05$ ; Fig. 3, *A* and *B*). These findings indicate that CsA treatment increases AKT activation and decreases PTEN levels in keratinocytes.

To determine whether the increased AKT activation is FBS-specific or is also hyperactivated in response to UVB radiation, we starved vehicle- or CsA-treated cells with 0.1% FBS for 24 h to eliminate serum effect. Then the starved cells were exposed to UVB radiation (20 mJ/cm<sup>2</sup>). This UVB dose was selected because it is the lowest dose inducing apoptosis of human HaCaT keratinocytes (Fig. 2*B*). UVB induced AKT activation at 1.5 and 3 h post-exposure. CsA treatment at 100 and 250 ng/ml significantly enhanced UVB-induced AKT phosphorylation at both time points ( $p < 0.05$ ), whereas CsA at 1000 ng/ml had no effect on UVB-induced AKT activation (Fig. 3, *C* and *D*). These data demonstrate that the effect of CsA on UVB-induced AKT activation is CsA-dose dependent; the clinical therapeutic CsA plasma levels (100 and 250 ng/ml) increase AKT activation, whereas the higher concentration (1000 ng/ml) does not. To further characterize the molecular effect of CsA, we determined whether CsA has a similar effect on the activation of EGFR, the AKT upstream pathway, and the activation of ERK as EGFR downstream. UVB radiation induced a slight increase in EGFR phosphorylation; CsA at 100 or 250 ng/ml had no effect on UVB-induced EGFR phosphorylation, whereas CsA at 1000 ng/ml dramatically increased EGFR phosphorylation. UVB activated ERK, whereas CsA treatment reduced ERK phosphorylation. It seems that at 1000 ng/ml CsA-induced EGFR activation is disconnected with AKT signaling and ERK pathway (Fig. 3*C*).

To analyze the effect of CsA on UVB-induced AKT activation at later times, we collected cells at 1.5, 6, and 24 h post-UVB radiation. We found that CsA significantly increased AKT phosphorylation at both serine 473 and threonine 308 ( $p < 0.05$ ; Fig. 3, *E* and *F*). These data indicate that AKT and PTEN are the molecular targets of CsA.

There are three AKT isoforms: AKT1, AKT2, and AKT3 (26). AKT3 expression is low in epidermis, whereas AKT1 and AKT2 are expressed (27). Using specific antibodies for each isoform to immunoprecipitate AKT1, AKT1/2/3 (AKT), AKT2, and AKT3, we found that, consistent with previous studies (27), AKT1 is the dominant isoform constituting 85% of total AKT (Fig. 3*G*). Only about 15% AKT was AKT2, whereas no AKT3 was detected. Similarly, AKT1 is the major isoform to be phosphorylated at serine 473 and threonine 308 under normal growth condition. CsA significantly increased AKT1 phosphorylation at serine 473 and threonine 308 ( $p < 0.05$ ; Fig. 3, *H* and *I*).

We could not detect AKT2 phosphorylation.

**PTEN Down-regulation Enhances UVB-induced AKT Activation in CsA-treated Cells**—It is known that PTEN deficiency causes increased AKT activation (28, 29). To determine the role of PTEN down-regulation in AKT activation, we first knocked down PTEN using small interfering RNA (RNAi) targeting PTEN (iPTEN) and then exposed the cells to UVB. Negative control (NC) siRNA was used as a transfection control. UVB induced AKT activation in NC-transfected cells. PTEN knock-down had little effect on AKT activation at 1.5 h (data not shown), whereas it dramatically increased AKT activation at 3 h and up to 24 h post-UVB (Fig. 4*A*).

To rule out off-target effect of RNAi, we used two independent short hairpin RNAs (i-1 and i-2) targeting PTEN at different sequences. HeLa cells were used, because much higher transfection efficiency can be achieved from these cells than from HaCaT or other keratinocytes. We found that both i-1 and i-2 effectively knocked down PTEN (Fig. 4*B*). At 24 h post-UVB, AKT phosphorylation (at serine 473) was significantly higher in i-1- and i-2-transfected cells than in NC-transfected cells ( $p < 0.05$ ). Thus, we confirmed that PTEN down-regulation increases UVB-induced AKT activation.

When we increased PTEN levels in CsA-treated cells using an adenoviral vector expressing wild-type PTEN, AKT phosphorylation (at serine 473) was significantly reduced ( $p < 0.05$ ; Fig. 4, *C* and *D*), demonstrating the critical role of CsA-induced PTEN suppression in enhancing UVB-induced AKT activation.

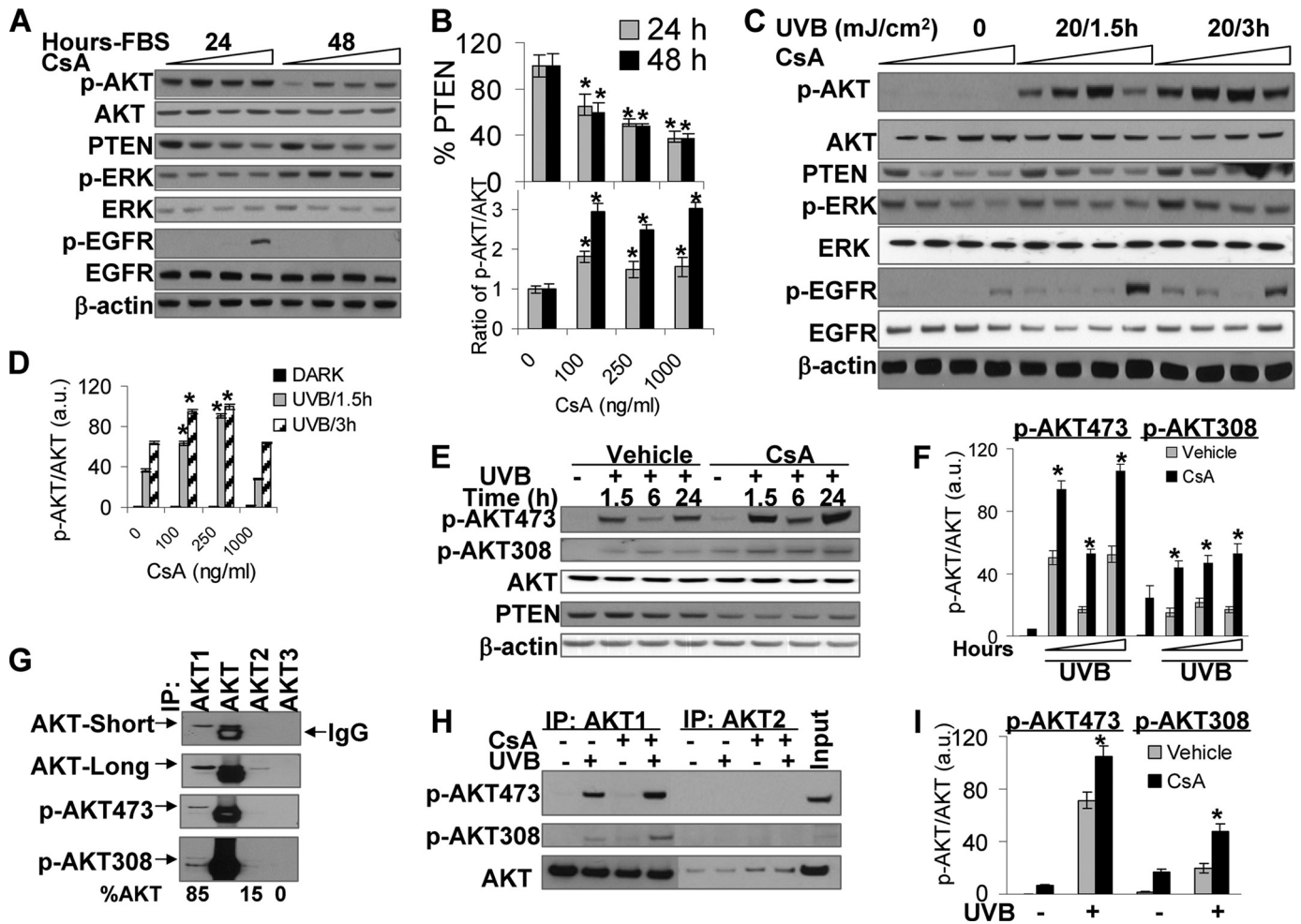


**FIGURE 3. CsA treatment increased AKT phosphorylation and decreased PTEN levels.** *A*, HaCaT cells treated with vehicle or CsA were incubated with fresh medium with 10% FBS. Then cells were collected at 24 or 48 h. Cell lysates were analyzed by immunoblotting with antibodies specific for phospho-AKT473 (p-AKT), phospho-ERK (p-ERK), phospho-EGFR, EGFR, ERK, AKT, PTEN, or  $\beta$ -actin as an equal loading control. *B*, shown is quantification of PTEN levels and AKT phosphorylation. *C*, cells were starved with 0.1% FBS for 24 h to remove serum effect. Cells were then exposed to UVB (20 mJ/cm<sup>2</sup>) and collected at 1.5 or 3 h after UVB radiation. Cell lysates were analyzed as in *A*. *D*, shown is quantification of p-AKT/AKT. *a.u.*, arbitrary units. *E*, cells were exposed to UVB as in *C* and then incubated for 1.5, 6, or 24 h. Cells were collected and analyzed by immunoblotting as in *A* with antibodies specific for p-AKT473, phospho-AKT308 (p-AKT308), AKT, PTEN, or  $\beta$ -actin (as an equal loading control). *F*, quantification of p-AKT473/AKT and p-AKT308/AKT is shown. *G*, HaCaT cell lysates were incubated with AKT1, AKT1/2/3 (AKT), AKT2, and AKT3 antibodies to pull down these proteins. Their levels in the pull-down assay were measured by immunoblotting using anti-AKT1/2/3, anti-p-AKT473, and anti-phospho-AKT308 antibodies. *IP*, immunoprecipitation. Percentage (%) of each isoform in total AKT was shown at the bottom. *H*, cells were exposed to UVB (20 mJ/cm<sup>2</sup>) and collected at 1.5 h. Cell lysates were incubated with anti-AKT1 and anti-AKT2 antibodies to pull down AKT1 and AKT2. p-AKT473, p-AKT308, and total AKT were determined by immunoblotting as in *G*. Total cell lysate from UVB-irradiated cells without CsA treatment was used as an input. *I*, quantification of p-AKT473/AKT and p-AKT308/AKT was as in *H*. \*,  $p < 0.05$ , significant difference from cells treated without CsA.

Upstream pathways including EGFR and PI3K are critical for AKT activation (26). To determine whether these pathways are required for CsA-enhanced AKT activation, we preincubated cells with the specific EGFR kinase inhibitor AG (1  $\mu$ M) or the specific PI3K inhibitor LY (10  $\mu$ M). Higher AKT activation was seen in CsA-treated cells than vehicle-treated cells (Fig. 4E). Either AG or LY inhibited both basal and CsA-induced AKT activation, indicating that CsA-enhanced AKT activation requires EGFR and PI3K activity.

**CsA Down-regulates PTEN in Mouse Skin and in A431 Cells—**To determine whether CsA-induced PTEN down-regulation is specific for HaCaT cells, we determined the effect of CsA on PTEN levels in mouse epidermis and in A431 epidermoid SCC cells. To minimize the possible role of immunosuppression, we used nude mice. We used immunohistochemistry

and Western analysis to measure PTEN protein levels in mouse epidermis. Daily CsA (20 mg/kg of body weight) for 30 days significantly down-regulated PTEN protein levels in basal (as indicated by *arrow*) and suprabasal keratinocytes (Fig. 5, A and B). This significant PTEN down-regulation was further confirmed by Western analysis ( $p < 0.05$ ; Fig. 5, C and D).

To further test the hypothesis that PTEN is down-regulated by CsA in keratinocytes, we determined the effect of CsA on PTEN in A431 epidermoid cells. CsA treatment significantly suppressed PTEN levels after 4 weeks ( $p < 0.05$ ; Fig. 5, E and F) but not 1 week. In parallel, CsA treatment for 4 weeks significantly increased AKT phosphorylation but not EGFR phosphorylation ( $p < 0.05$ ; Fig. 5, E and G). Therefore, we confirmed that CsA treatment down-regulates the tumor suppressor PTEN in epidermal keratinocytes.

## Cyclosporin A Activates AKT

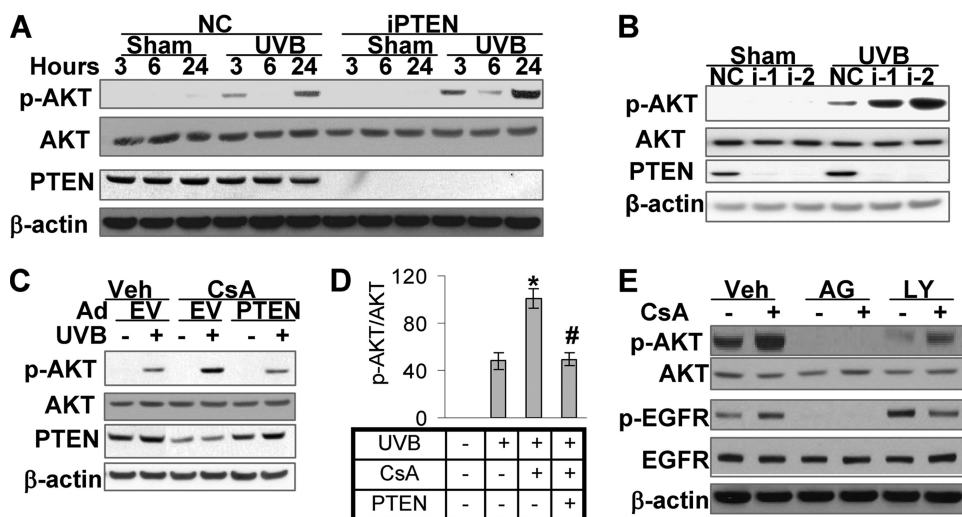


**FIGURE 4. PTEN suppression is critical for CsA-enhanced AKT activation.** Western blotting was used to determine PTEN, p-AKT (serine 473), total AKT, and  $\beta$ -actin (as an equal loading control) as in Fig. 3. *A*, HaCaT cells were transfected with siRNA targeting PTEN (*iPTEN*) or NC. Cells were then exposed to UVB (20 mJ/cm<sup>2</sup>) and collected at 3, 6, and 24 h. *B*, HeLa cells were transfected with short hairpin RNA targeting PTEN or NC and then exposed to UVB as in *A*. Cells were collected at 24 h for Western analysis. *i-1* and *i-2* were two different shRNAs targeting different sequences of the PTEN gene. *C*, HaCaT cells treated with vehicle or CsA were infected with an adenoviral vector expressing PTEN or EV. Cells were then exposed to UVB as in *A* and then collected at 1.5 h for Western analysis. *D*, shown is quantification of p-AKT/AKT in *C*. *E*, cells treated with or without CsA were treated with the EGFR kinase inhibitor AG (1  $\mu$ M) or the specific PI3K inhibitor LY (10  $\mu$ M) for 1 h. *Veh*, vehicle. Then cells were collected for Western analysis. \*,  $p < 0.05$ , significant difference from cells treated without CsA. #,  $p < 0.05$ , significant difference from cells without PTEN overexpression.

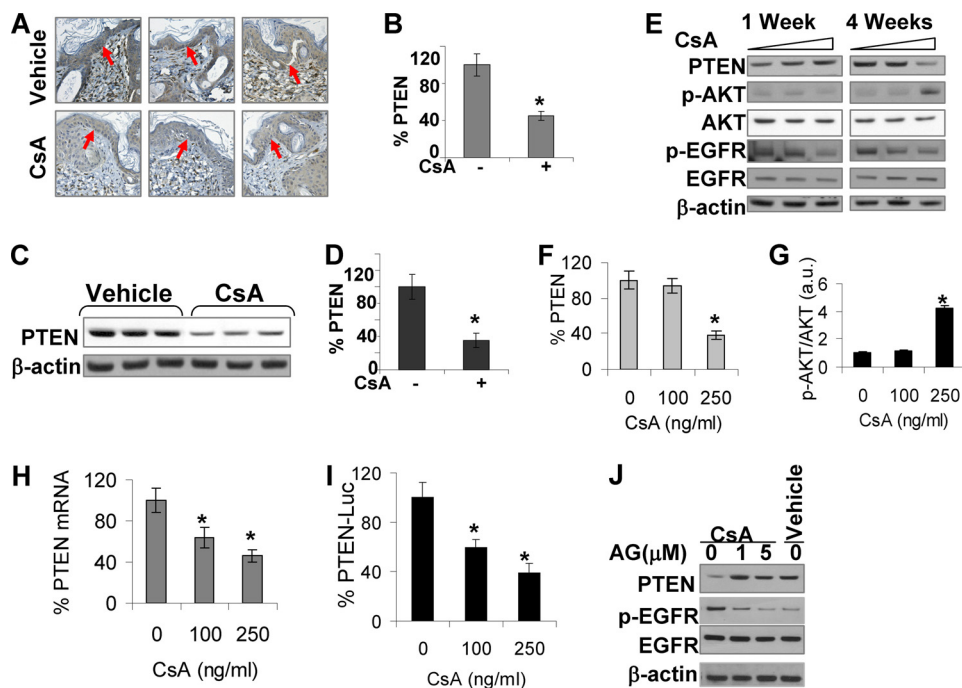


**FIGURE 5. CsA suppresses PTEN expression in mouse skin and A431 cells, and such PTEN suppression involves down-regulation of PTEN transcription and EGFR pathway.** *A*, immunohistochemical staining for PTEN in epidermis is shown. Nude mice ( $n = 3$ ) were treated with CsA (20 mg/kg of body weight) daily for 30 days or vehicle (olive oil). Skin was collected and analyzed for PTEN levels. The *arrow* indicates the basal keratinocytes to be used for quantification of PTEN levels. *B*, quantification of PTEN levels in *A* is shown. *C*, immunoblot analysis of PTEN levels in nude mouse skin with or without CsA treatment as in *A* is shown. *D*, shown is quantification of PTEN levels in *C*. *E*, A431 cells were treated with CsA (0, 100, or 250 ng/ml) for 1 and 4 weeks and collected for immunoblot analysis for PTEN, p-AKT, AKT, p-EGFR, EGFR, and  $\beta$ -actin as an equal loading control as in Fig. 3. *F*, quantification of PTEN levels in *E* is shown. *G*, quantification of p-AKT/AKT in *E* is shown. *H*, PTEN mRNA levels were determined by real-time PCR in vehicle and CsA-treated cells. *I*, shown is a reporter assay using PTEN promoter reporter of vehicle and CsA-treated cells. Luciferase activity was analyzed by dual luciferase reporter assay. *J*, shown is an immunoblot analysis of PTEN, p-EGFR, EGFR, and  $\beta$ -actin in CsA-treated cells at 72 h post-AG (0, 1, 5  $\mu$ M). Vehicle-treated cells were used as a comparison control. \*,  $p < 0.05$ , significant difference from mice or cells treated without CsA.

*CsA Down-regulates PTEN at the Transcription Level and in an EGFR-dependent Manner*—To determine the mechanisms of CsA-induced PTEN reduction, we examined the involvement of alterations in PTEN mRNA levels and transcription. CsA treatment (100 and 250 ng/ml) significantly reduced PTEN mRNA levels (Fig. 5*H*). To further explore whether this PTEN suppression is mediated at the transcription level, we determined PTEN promoter transcription activity using a reporter assay. CsA significantly suppressed PTEN promoter activity (Fig. 5*I*). These findings demonstrate that CsA down-regulates PTEN transcription.

To determine the molecular mechanisms, we analyzed the role of EGFR pathway in CsA-induced PTEN down-regulation. When CsA-treated cells were incubated with the EGFR kinase inhibitor AG (1 and 5  $\mu$ M) for 72 h, PTEN levels were significantly increased (Fig. 5*J*,  $p < 0.05$ ). Thus, EGFR pathway is critical for CsA-induced PTEN down-regulation.

*AKT Activation Is Required for CsA-induced Resistance to Apoptosis Induced by UVB and Growth*—The AKT pathway plays critical roles in cell survival and growth (26). To determine whether AKT activation enhanced by CsA treatment protects cells from UVB-induced apoptosis, we pretreated CsA- or vehicle-treated cells with the specific PI3K/AKT inhibitor LY (10  $\mu$ M) for 1 h and then exposed the cells to UVB (30 mJ/cm<sup>2</sup>). Fourteen hours after UVB radiation, we collected the cells and analyzed apoptosis as described in Fig. 2*C*. Inhibiting AKT activation by LY induced apoptosis in cells kept in the dark (Fig. 6*A*), demonstrating that AKT signaling is critical for cell survival in cells without UVB radiation. CsA treatment reduced apoptosis induced by UVB radiation. However, LY significantly increased apoptosis in both CsA-treated and untreated cells upon UVB radiation ( $p < 0.05$ ). It appears that more CsA-treated cells underwent apoptosis after UVB radiation when AKT

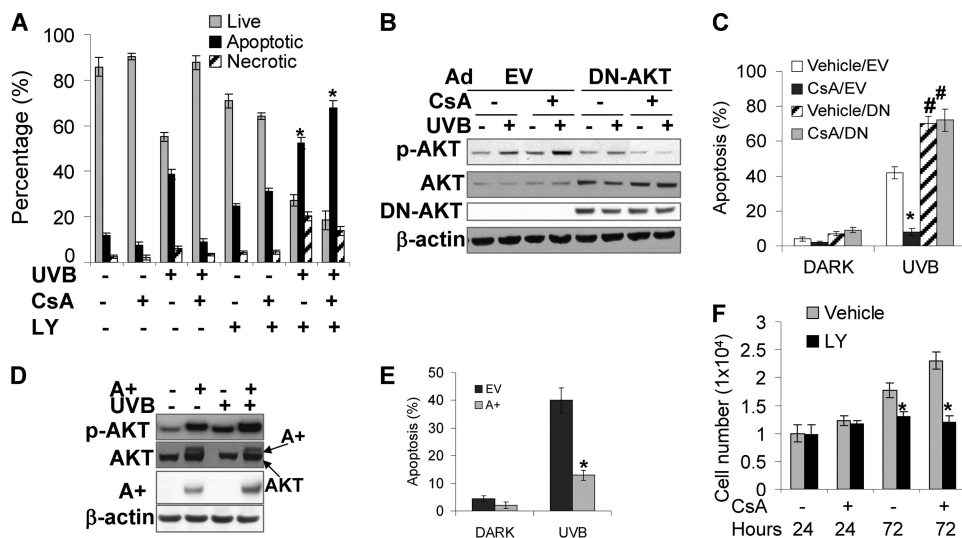


**FIGURE 6. AKT activation is essential to promote survival and growth of keratinocytes treated with or without CsA upon UVB radiation.** *A*, cells treated with or without CsA (250 ng/ml) as in Fig. 1 were incubated with the specific PI3K inhibitor LY (10  $\mu$ M) and then exposed to UVB (30 mJ/cm<sup>2</sup>). Fourteen hours after UVB radiation, we collected the cells and analyzed apoptosis as described in Fig. 2A. \*,  $p < 0.05$ , significant difference from cells treated without LY. *B*, cells were infected with an adenoviral vector expressing dominant-negative AKT (DN-AKT) or EV and then exposed to UVB (20 mJ/cm<sup>2</sup>). Cells were collected at 1.5 h for immunoblotting analysis as in Fig. 3. Expression of DN-AKT was monitored by immunoblot using anti-hemagglutinin antibody. *C*, cells were infected as in *B* with dominant-negative AKT. Cells were exposed to UVB and collected for apoptosis analysis as in Fig. 2A. \*,  $p < 0.05$ , significant difference from cells treated without CsA. #,  $p < 0.05$ , significant difference from cells treated without LY. *D*, HaCaT cells were infected with an adenoviral vector expressing constitutively active AKT (A+) or EV. Cells were then exposed to UVB as in *B* and collected at 1.5 h for immunoblot analysis for p-AKT (serine 473), total AKT, and  $\beta$ -actin. Expression of A+ was monitored by immunoblot using anti-hemagglutinin antibody. *E*, cells were infected as in *D*. Cells were then exposed to UVB and collected for apoptosis analysis as in *C*. *F*, cells were seeded as in Fig. 1G. Twenty-four hours later cells were treated with LY (10  $\mu$ M) for 24 and 72 h. Cell growth was determined by MTS assay. \*,  $p < 0.05$ , significant difference from cells treated without LY.

pathway was inhibited, suggesting that CsA-treated cells highly depend on AKT activation for cell survival under UVB stress.

To further elucidate the role of AKT activation, we infected cells with an adenoviral vector expressing dominant negative AKT (DN-AKT) to inhibit AKT activation (30). DN-AKT expression inhibited UVB-induced AKT phosphorylation (at serine 473) in vehicle- and CsA-treated HaCaT cells, whereas empty vector (EV) had no effect (Fig. 6B). CsA significantly inhibited UVB-induced apoptosis ( $p < 0.05$ ), whereas DN-AKT increased it in both vehicle- and CsA-treated cells ( $p < 0.05$ ; Fig. 6C). To further determine the role of AKT activation in survival, we infected vehicle-treated HaCaT cells with constitutively active AKT (A+, Myr-AKT) to increase AKT activation. The antibodies for total AKT detected Myr-AKT, which migrated slightly slower than endogenous AKT (Fig. 6D) (31). Compared with EV, A+ also enhanced AKT phosphorylation in cells exposed to UVB and sham-irradiated (Fig. 6D). Increased AKT activation significantly reduced UVB-induced apoptosis ( $p < 0.05$ ; Fig. 6E). Therefore, these findings demonstrate that AKT activation enhances cell survival upon UVB damage.

To determine whether AKT activation plays an active role in CsA-promoted cell growth, we treated the cells with LY (10  $\mu$ M) for 24 and 72 h. Although LY had no effect on cell growth at 24 h, it significantly inhibited cell growth at 72 h in both vehicle- and CsA-treated cells ( $p < 0.05$ ; Fig. 6F). Taking together, CsA-enhanced AKT activation promotes both cell survival and growth.

*mTOR Signaling Is Critical for CsA-mediated Survival and Growth*—mTOR is a downstream pathway of AKT and plays a critical role in skin tumorigenesis (32). To delineate the mechanism by which AKT affects survival and growth, we assessed the role of mTOR as a downstream effector. Inhibition of mTOR with rapamycin (10 or 20  $\mu$ M) significantly increased UVB-induced apoptosis in vehicle- and CsA-treated HaCaT cells ( $p < 0.05$ ; Fig. 7A). Rapamycin at either concentration abolished the anti-apoptotic effect of CsA. In addition, more cells underwent apoptosis upon UVB radiation when mTOR was inhibited. Using a viability assay, in vehicle- and CsA-treated cells we found that rapamycin significantly reduced cell survival after UVB irradiation ( $p < 0.05$ ; Fig. 7B). Thus, our results indicate that CsA-treated cells highly depend on mTOR signaling for cell survival after UVB damage.

To determine the role of mTOR signaling in CsA-promoted growth, we incubated cells with different

concentrations of rapamycin (0, 2, 5, 10, and 20  $\mu$ M) for 24 and 72 h. Rapamycin had no significant effect at 24 h, whereas at 72 h, CsA significantly inhibited growth of vehicle- and CsA-treated HaCaT cells ( $p < 0.05$ ; Fig. 7C). These data demonstrate that mTOR signaling is essential for CsA-enhanced cell survival from UVB damage and growth.

## DISCUSSION

CsA has been widely used to prevent graft rejection in organ transplantation. The mechanism of CsA action in causing skin cancer was thought to be well understood via immunosuppression. However, the marginal increase (1–3-fold) of skin cancer in AIDS patients depending on geographical regions (33–38) does not support the mechanisms of immune surveillance in skin carcinogenesis. Recent evidence has indicated that CsA increases metastasis of lung cancer cells in nude mice that have no immune system for CsA to suppress (39). Yarosh *et al.* (40) have demonstrated that CsA at 1  $\mu$ g/ml reduce the repair of UVB-induced DNA damage and inhibit apoptosis in human keratinocytes through inhibiting nuclear factor of activated T-cells (NFAT). Here we have shown that chronic treatment of human HaCaT keratinocytes with CsA at therapeutic plasma levels (100 and 250 ng/ml (23)) promotes growth and survival from loss of extracellular matrix and UVB radiation. CsA enhances AKT activation through suppressing PTEN. Our studies identified PTEN/AKT pathways as the new molecular targets of CsA in epidermal keratinocytes.

## Cyclosporin A Activates AKT

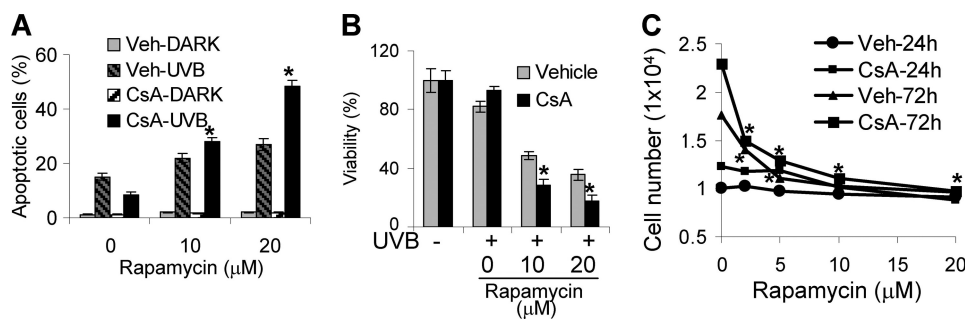


**FIGURE 7. mTOR signaling plays a critical role in CsA-promoted survival and growth of keratinocytes.** A, cells were treated with the mTOR inhibitor rapamycin (0, 10, or 20  $\mu\text{M}$ ) for 1 h. Cells were then exposed to UVB and collected for apoptosis analysis as in Fig. 2C. B, cells were treated as in A and collected for viability analysis by MTS assay. C, cells were seeded as in Fig. 1G and then treated with rapamycin at different concentrations. Cells were then collected for growth analysis by MTS assay. \*,  $p < 0.05$ , significant difference from cells treated without rapamycin. Veh, vehicle.

CsA promotes cell survival and growth *in vitro* and tumor growth of human epidermoid squamous cell carcinoma A431 cells *in vivo* in immune-deficient nude mice after subcutaneous injection. Our findings indicate immunosuppression-independent mechanisms that act on the keratinocytes by activating oncogenes, inactivating tumor suppressors, or both.

At the molecular level, CsA increases AKT activation that is required for cell survival and growth. An increased survival has been seen in CsA-treated lung cancer cells (39). As UVB radiation in sunlight is a major risk factor causing skin cancer in humans, apoptosis of keratinocytes after UVB radiation has been considered to be cancer-preventive through eliminating damaged cells. Consistent with previous studies (40), our data indicate that CsA treatment inhibits UVB-induced apoptosis. Inhibiting AKT activation by the specific PI3K inhibitor LY294002 abolished the enhancing effect of CsA on survival and growth.

CsA treatment down-regulates the tumor suppressor and AKT-antagonizing protein PTEN in both HaCaT and A431 cells *in vitro* and in mouse epidermis *in vivo*. Such PTEN reduction in CsA-treated cells enhanced AKT activation, because 1) increasing PTEN levels in CsA-treated cells inhibited AKT activation and 2) knock-down PTEN enhanced AKT activation after UVB irradiation. In addition, EGFR and PI3K activation is required for the basal and CsA-induced AKT activation. CsA-enhanced AKT activation post-UVB may also involve EGFR and PI3K activation (4, 8).

We found that CsA-induced PTEN down-regulation was at the transcription level and was EGFR-dependent. It is possible that EGFR downstream pathways including Ras activation mediate CsA-induced PTEN down-regulation (41). We are currently continuing to elucidate the molecular mechanisms of CsA-induced PTEN suppression in keratinocytes in detail.

It seems that the mTOR pathway as an AKT downstream signal plays a critical role in CsA-promoted growth and survival of keratinocytes. In fact, it has shown that the mTOR inhibitor rapamycin, a new immunosuppressive drug, antagonizes skin tumorigenesis in hairless mice first exposed to UVB and then treated CsA (42).

As a critical downstream target of AKT activation, mTOR plays critical roles in cell growth and survival, and AKT/mTOR have been considered as a targets for cancer therapy (43–45).

Recent studies have shown that rapamycin inhibits primary and metastatic tumor growth of murine colon cancer, melanoma, or renal cancer cells in mice, whereas CsA promotes metastasis of these cancer cells (46–48). The opposing effects of rapamycin and CsA observed in these studies unlink immunosuppression from tumorigenesis and tumor progression. The combination of CsA and rapamycin for immunosuppression for organ transplant recipients has been proposed to reduce cancer burden in these individuals. However, the high

wound healing complication rates after kidney transplantation (49) and tracheal anastomosis complication after lung transplantation (50) may limit the clinical application of rapamycin immediately after transplantation. Animal studies have shown that rapamycin impairs all steps of the wound healing process (51). Better strategies targeting PTEN/AKT are needed to reduce the oncogenic effect of CsA.

Our studies not only identify PTEN/AKT as new molecular targets of CsA in epidermal keratinocytes but also provide promise for preventing and treating skin cancer in CsA-treated organ transplant patients. Better preventive and therapeutic agents are urgently needed. Targeting PTEN/AKT pathways in combination with sun protection may provide hope to reduce the skin cancer burden in these patients.

*Acknowledgments*—We are grateful to Dr. Kenneth Walsh (Boston University) for the adenoviral vectors expressing dominant-negative AKT and constitutively active AKT, Dr. Christopher Kontos for the adenoviral PTEN vector and empty vector, and Dr. William Hahn for PTEN shRNA.

## REFERENCES

- Jensen, P., Hansen, S., Møller, B., Leivestad, T., Pfeffer, P., Geiran, O., Fauchald, P., and Simonsen, S. (1999) *J. Am. Acad. Dermatol.* **40**, 177–186
- Berg, D., and Otley, C. C. (2002) *J. Am. Acad. Dermatol.* **47**, 1–17; quiz 18–20
- Euvrard, S., Kanitakis, J., and Claudy, A. (2003) *N. Engl. J. Med.* **348**, 1681–1691
- Bode, A. M., and Dong, Z. (2003) *Sci. STKE* 2003, RE2
- de Gruijff, F. R., Sterenborg, H. J., Forbes, P. D., Davies, R. E., Cole, C., Kelfkens, G., van Weelden, H., Slaper, H., and van der Leun, J. C. (1993) *Cancer Res.* **53**, 53–60
- Noonan, F. P., Recio, J. A., Takayama, H., Duray, P., Anver, M. R., Rush, W. L., De Fabo, E. C., and Merlino, G. (2001) *Nature* **413**, 271–272
- Setlow, R. B., Grist, E., Thompson, K., and Woodhead, A. D. (1993) *Proc. Natl. Acad. Sci. U.S.A.* **90**, 6666–6670
- Bowden, G. T. (2004) *Nat. Rev. Cancer* **4**, 23–35
- Kraemer, K. H. (1997) *Proc. Natl. Acad. Sci. U.S.A.* **94**, 11–14
- Wishart, M. J., and Dixon, J. E. (2002) *Trends Cell Biol.* **12**, 579–585
- Maehama, T., Taylor, G. S., and Dixon, J. E. (2001) *Annu. Rev. Biochem.* **70**, 247–279
- Di Cristofano, A., and Pandolfi, P. P. (2000) *Cell* **100**, 387–390
- Liaw, D., Marsh, D. J., Li, J., Dahia, P. L., Wang, S. I., Zheng, Z., Bose, S., Call, K. M., Tsou, H. C., Peacocke, M., Eng, C., and Parsons, R. (1997) *Nat. Genet.* **16**, 64–67



14. Suzuki, A., Itami, S., Ohishi, M., Hamada, K., Inoue, T., Komazawa, N., Senoo, H., Sasaki, T., Takeda, J., Manabe, M., Mak, T. W., and Nakano, T. (2003) *Cancer Res.* **63**, 674–681
15. He, Y. Y., Pi, J., Huang, J. L., Diwan, B. A., Waalkes, M. P., and Chignell, C. F. (2006) *Oncogene* **25**, 3680–3688
16. He, Y. Y., Council, S. E., Feng, L., and Chignell, C. F. (2008) *Cancer Res.* **68**, 3752–3758
17. He, Y. Y., Huang, J. L., and Chignell, C. F. (2006) *Oncogene* **25**, 1521–1531
18. Kim, H. K., Zhang, H., Li, H., Wu, T. T., Swisher, S., He, D., Wu, L., Xu, J., Elmets, C. A., Athar, M., Xu, X. C., and Xu, H. (2008) *Neoplasia* **10**, 1411–1420
19. He, Y. Y., Council, S. E., Feng, L., Bonini, M. G., and Chignell, C. F. (2008) *Photochem. Photobiol.* **84**, 69–74
20. Boehm, J. S., Hession, M. T., Bulmer, S. E., and Hahn, W. C. (2005) *Mol. Cell. Biol.* **25**, 6464–6474
21. Sumitomo, M., Iwase, A., Zheng, R., Navarro, D., Kamnietzky, D., Shen, R., Georgescu, M. M., and Nanus, D. M. (2004) *Cancer Cell* **5**, 67–78
22. He, Y. Y., Huang, J. L., Sik, R. H., Liu, J., Waalkes, M. P., and Chignell, C. F. (2004) *J. Invest. Dermatol.* **122**, 533–543
23. Dantal, J., Hourmant, M., Cantarovich, D., Giral, M., Blanco, G., Dreno, B., and Souillou, J. P. (1998) *Lancet* **351**, 623–628
24. Lehman, T. A., Modali, R., Boukamp, P., Stanek, J., Bennett, W. P., Welsh, J. A., Metcalf, R. A., Stampfer, M. R., Fusenig, N., Rogan, E. M., et al. (1993) *Carcinogenesis* **14**, 833–839
25. Nakazawa, H., English, D., Randell, P. L., Nakazawa, K., Martel, N., Armstrong, B. K., and Yamasaki, H. (1994) *Proc. Natl. Acad. Sci. U.S.A.* **91**, 360–364
26. Datta, S. R., Brunet, A., and Greenberg, M. E. (1999) *Genes Dev.* **13**, 2905–2927
27. Goren, I., Müller, E., Schiefelbein, D., Gutwein, P., Seitz, O., Pfeilschifter, J., and Frank, S. (2009) *J. Invest. Dermatol.* **129**, 752–764
28. Maehama, T., and Dixon, J. E. (1998) *J. Biol. Chem.* **273**, 13375–13378
29. Stambolic, V., Suzuki, A., de la Pompa, J. L., Brothers, G. M., Mirtsos, C., Sasaki, T., Ruland, J., Penninger, J. M., Siderovski, D. P., and Mak, T. W. (1998) *Cell* **95**, 29–39
30. Fujio, Y., Guo, K., Mano, T., Mitsuchi, Y., Testa, J. R., and Walsh, K. (1999) *Mol. Cell. Biol.* **19**, 5073–5082
31. Shair, K. H., Schnegg, C. I., and Raab-Traub, N. (2008) *Cancer Res.* **68**, 6997–7005
32. Skeen, J. E., Bhaskar, P. T., Chen, C. C., Chen, W. S., Peng, X. D., Nogueira, V., Hahn-Windgassen, A., Kiyokawa, H., and Hay, N. (2006) *Cancer Cell* **10**, 269–280
33. Dal Maso, L., Polesel, J., Serraino, D., Lise, M., Piselli, P., Falcini, F., Russo, A., Intriери, T., Vercelli, M., Zambon, P., Tagliabue, G., Zanetti, R., Federico, M., Limina, R. M., Mangone, L., De Lisi, V., Stracci, F., Ferretti, S., Piffer, S., Budroni, M., Donato, A., Giacomini, A., Bellù, F., Fusco, M., Madeddu, A., Vitarelli, S., Tessandori, R., Tumino, R., Suligo, B., and Franceschi, S. (2009) *Br. J. Cancer* **100**, 840–847
34. Engels, E. A., Pfeiffer, R. M., Goedert, J. J., Virgo, P., McNeel, T. S., Scoppa, S. M., and Biggar, R. J. (2006) *AIDS* **20**, 1645–1654
35. Engels, E. A., Biggar, R. J., Hall, H. L., Cross, H., Crutchfield, A., Finch, J. L., Grigg, R., Hylton, T., Pawlish, K. S., McNeel, T. S., and Goedert, J. J. (2008) *Int. J. Cancer* **123**, 187–194
36. Goedert, J. J., Coté, T. R., Virgo, P., Scoppa, S. M., Kingma, D. W., Gail, M. H., Jaffe, E. S., and Biggar, R. J. (1998) *Lancet* **351**, 1833–1839
37. Allardice, G. M., Hole, D. J., Brewster, D. H., Boyd, J., and Goldberg, D. J. (2003) *Br. J. Cancer* **89**, 505–507
38. Clifford, G. M., Polesel, J., Rickenbach, M., Dal Maso, L., Keiser, O., Kofler, A., Rapiti, E., Levi, F., Jundt, G., Fisch, T., Bordoni, A., De Weck, D., and Franceschi, S. (2005) *J. Natl. Cancer Inst.* **97**, 425–432
39. Hojo, M., Morimoto, T., Maluccio, M., Asano, T., Morimoto, K., Lagman, M., Shimbo, T., and Suthanthiran, M. (1999) *Nature* **397**, 530–534
40. Yarosh, D. B., Pena, A. V., Nay, S. L., Canning, M. T., and Brown, D. A. (2005) *J. Invest. Dermatol.* **125**, 1020–1025
41. Vasudevan, K. M., Burikhanov, R., Goswami, A., and Rangnekar, V. M. (2007) *Cancer Res.* **67**, 10343–10350
42. Wulff, B. C., Kusewitt, D. F., VanBuskirk, A. M., Thomas-Ahner, J. M., Duncan, F. J., and Oberyszyn, T. M. (2008) *J. Invest. Dermatol.* **128**, 2467–2473
43. Chang, F., Lee, J. T., Navolanic, P. M., Steelman, L. S., Shelton, J. G., Blalock, W. L., Franklin, R. A., and McCubrey, J. A. (2003) *Leukemia* **17**, 590–603
44. Tsang, C. K., Qi, H., Liu, L. F., and Zheng, X. F. (2007) *Drug Discov. Today* **12**, 112–124
45. Vignot, S., Favre, S., Aguirre, D., and Raymond, E. (2005) *Ann. Oncol.* **16**, 525–537
46. Guba, M., von Breitenbuch, P., Steinbauer, M., Koehl, G., Flegel, S., Hornung, M., Bruns, C. J., Zuelke, C., Farkas, S., Anthuber, M., Jauch, K. W., and Geissler, E. K. (2002) *Nat. Med.* **8**, 128–135
47. Luan, F. L., Ding, R., Sharma, V. K., Chon, W. J., Lagman, M., and Suthanthiran, M. (2003) *Kidney Int.* **63**, 917–926
48. Luan, F. L., Hojo, M., Maluccio, M., Yamaji, K., and Suthanthiran, M. (2002) *Transplantation* **73**, 1565–1572
49. Dean, P. G., Lund, W. J., Larson, T. S., Prieto, M., Nyberg, S. L., Ishitani, M. B., Kremers, W. K., and Stegall, M. D. (2004) *Transplantation* **77**, 1555–1561
50. Groetzner, J., Kur, F., Spelsberg, F., Behr, J., Frey, L., Bittmann, I., Vogeser, M., Ueberfuhr, P., Meiser, B., Hatz, R., and Reichart, B. (2004) *J. Heart Lung Transplant* **23**, 632–638
51. Ekici, Y., Emiroglu, R., Ozdemir, H., Aldemir, D., Karakayali, H., and Haberal, M. (2007) *Transplant. Proc.* **39**, 1201–1203